Accepted Manuscript

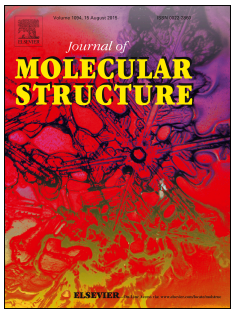

Synthesis, characterization and Al^{3+} sensing application of a new chromo-fluorogenic chemosensor

Xin Leng, Xu Jia, Chengfang Qiao, Wenfeng Xu, Chongting Ren, Ying Long, Bingqin Yang

PII: S0022-2860(19)30591-5

DOI: https://doi.org/10.1016/j.molstruc.2019.05.032

Reference: MOLSTR 26539

To appear in: *Journal of Molecular Structure*

Received Date: 22 December 2018

Revised Date: 9 May 2019

Accepted Date: 10 May 2019

Please cite this article as: X. Leng, X. Jia, C. Qiao, W. Xu, C. Ren, Y. Long, B. Yang, Synthesis, characterization and Al^{3+} sensing application of a new chromo-fluorogenic chemosensor, *Journal of Molecular Structure* (2019), doi: https://doi.org/10.1016/j.molstruc.2019.05.032.

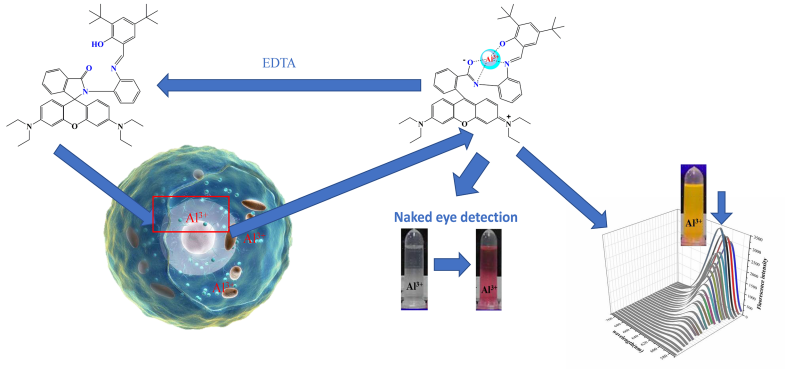

Synthesis, Characterization and Al^{3+} Sensing Application of a New Chromo-Fluorogenic Chemosensor

Xin Leng,[‡a] Xu Jia,[‡a] Chengfang Qiao,[b,*] Wenfeng Xu,[a] Chongting Ren,[a] Ying Long,[a] Bingqin Yang[a,*]

[a] *Key Laboratory of Synthetic and Natural Functional Molecule Chemistry of Ministry of Education, College of Chemistry and Materials Science, Northwest University, Xi'an 710127, China*

[b] *Shaanxi Key Laboratory of Comprehensive Utilization of Tailings Resources, College of Chemical Engineering and Modern Materials, Shangluo University, Shangluo 726000, China*

‡ Both authors contributed equally to this work

[*]Corresponding Authors: Prof. Bingqin Yang (E-mail address: organic_lengxin@163.com);
Prof. Chengfang Qiao (E-mail address: xiaoqiaoqcf@126.com)

Abstract

A rhodamine B-based chromo-fluorogenic probe **BOS** is prepared with a good yield by condensating an o-diaminobenzene functionalized rhodamine derivative (**RBO**) and a large steric hindrance salicylaldehyde, and characterized by elemental analysis, infrared spectroscopy (IR), ^{1}H and ^{13}C NMR technology, and high resolution mass spectrum (HRMS). Spectroscopy experiments reveal that the probe can selectively and sensitively detect Al^{3+} from a variety of metal ions with a low detection limit of 1.855 μmol/L. Compared to traditional detection methods, **BOS** provides an inexpensive, rapid and straightforward way for Al^{3+} detection that can be distinguished by "naked eye". The MTT (3-(4,5-dimethylthiazol-2-yl)-2,5-diphenyl-2-*H*- tetrazoliubromide) assays and cell imaging experiments demonstrate that the sensor is low toxic and amicable for Al^{3+} sensing in living cells.

Keywords: Rhodamine derivative; Fluorescence probe; Bioimaging; Al^{3+} Detection

1. Introduction

Aluminium, known as the maximum metallic element on the earth [1-5], has developed rapidly in the past decades. It is widely applied in daily routine ranging from water purification, aluminium-ion battery, packing materials, food additives [6-9]. Meanwhile, due to the accumulation of excessive ingestion, the damage of dissolved Al^{3+} in human body has received increasing attention from a number of different disciplines, among which medical research announces that Alzheimer's disease is caused by a typical neurofibril injury from aluminium [10, 11]. This promotes the invention to quantificationally analyze Al^{3+} in a fast and visible way. Technologies that concentrate on Al^{3+} detection more frequently adopt approaches like ^{27}Al NMR technology, atomic absorption spectrometry (AAS), inductively coupled plasma atomic emission spectrometry (ICP-AES), mass spectrometry and electrochemical methods, while most of them are complicated, time-consuming as well as expensive due to insufficient spectroscopic characteristics of Al^{3+} [12-16].

Fluorescence analysis, reported as a convenient, low cost, sensitive and quick response method [17], has promoted the developement of fluorescence sensing, and led to the emergence of a large number of effective and sensitive chemosensors. Given the inherent nature of aluminium ion such as poor bonding capacity and robust tendency to hydrolysis, micromolecular Al^{3+} fluorescent sensors with multidentate coordination sites and strong chromophore are highly promising. Therefore, among the "off-on" fluorescent sensors [18], rhodamine-based probes are highlighted because of their extraordinary photophysical properties like good photostability, relatively higher fluorescence quantum yield, excellent anti-interference capacity, advanced detection mechanism and special emission wavelength [19].

In this paper, a newly designed rhodamine-based probe **BOS** was obtained based on a three-step synthesis procedure (Scheme 1). In **BOS**, the flexible benzoic acid moeity of rhodamine B was substituted by the functional group with multidentate chelation sites to form the spirolactam form, which benefits to chelate target ions to display "turn-on" fluorescence signal by the conformational switching

from spirocyclic to open-cycle structure. Additionally, the large steric hindrance tertiary butyl groups were introduced on the salicylaldehyde functional group for trying to improve the sensing selectivity of **BOS**. This chemosensor can be utilized to detecte Al^{3+} in a naked-eye way through the fast and remarkable fluorescence enhancement and obvious colour variations. The outstanding characterizations of **BOS** endow it great potential applications for biological imaging [20-24].

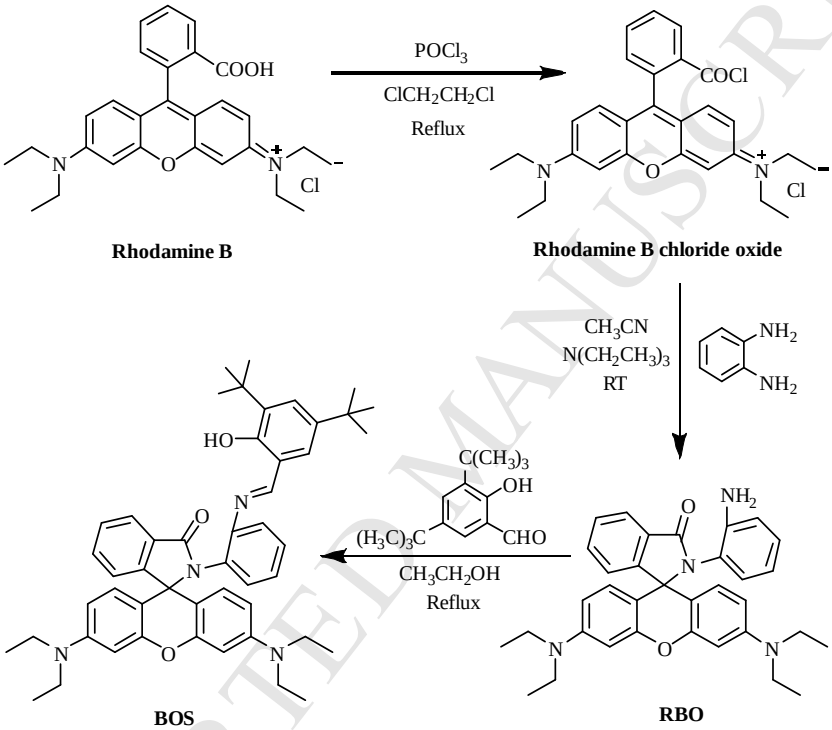

Scheme 1. Synthesis of **BOS**.

2. Experimental section

2.1. Materials and methods

All materials were purchased commercially without further purification. The **BOS** powders were dissolved in ethanol as stock solutions (1 mmol/L), which were taken quantificationally in different experiments. Fluorescence and absorbance spectra were performed on a HITACHI F-4500 fluorescence spectrophotometer and a

Shimadzu UV-1700 spectrophotometer, respectively. Elemental analyses for C, H, and N were determined on a Vario EL III elemental analyzer. Infrared spectrum was taken on a Bruker Tensor 27 spectrometer within the range of 4000-400 cm^{-1} by using KBr pellets. NMR spectra were obtained on a Varian INOVA-400 MHz spectrometer (at 100 MHz for ^{13}C NMR and at 400 MHz for ^{1}H NMR). A Bruker micro TOF-Q II ESI-TOF LC/MS/MS Spectroscopy was used to perform mass spectra. Melting point test was recorded on an XT-4 micromelting apparatus without corrected. Living cells imaging experiments were preformed on an Olympus FV1000 confocal microscopy. Cytotoxicity analysis was recorded with the Soft max pro software (version 2.2.1) in Spectra max190-Molecular Devices. Thermogravimetric analysis was investigated using a Netzsch STA 449C thermogravimetric analyzer.

2.2. Synthetic procedures

*2.2.1. Synthesis of the intermediate product **RBO***

$POCl_3$ (1 mL, 10 mmol) was added to a 30 mL 1,2-dichloroethane solution of rhodamine B (1.60 g, 3 mmol), the reaction mixture was refluxed for 8 h. After cooling to ambient temperature, the solvent was removed under reduced pressure, and the residue directly reacted with o-phenylenediamine (0.32 g, 3 mmol) in CH_3CN. 30 min later, triethylamine (1 mL) was added into the resulting mixture, and stirred for 10 h. After removal of the solvent under reduced pressure, the crude product was purified by silica gel column chromatography to give **RBO** in 89.2% yield. The high resolution mass spectrum (HRMS) analysis for **RBO** ($C_{34}H_{36}N_4O_2$): Calculated: *m/z* = 532.2838, Found: 533.2897 $(M+H)^+$ (Fig. S1). ^{1}H NMR (400 M, $CDCl_3$), δ: 8.07–8.09 (d, *J* = 8 Hz, 1H), 7.57–7.62 (q, *J* = 8 Hz, 2H), 7.29–7.31 (d, *J* = 8 Hz, 1H), 6.98–7.01 (t, *J* = 4 Hz, 1H), 6.80–6.08 (m, 9H), 3.32–3.37 (dd, *J* = 8 Hz, 8H), 1.17–1.21 (t, *J* = 8 Hz, 12H) (Fig. S2).

*2.2.2. Synthesis of **BOS***

The intermediate **RBO** (0.53 g, 1 mmol) and 3,5-ditert-butyl salicylaldehyde

(0.23 g, 1 mmol) were dissolved in 40 mL ethanol solution, stirred and refluxed for 1 h at 80 °C. After cooling to room temperature, the beige precipitate was purified by recrystallization in ethanol/water to give **BOS** (beige powder) in 90.8% yield. Melting point: 157~158 ℃. Elemental analysis for $C_{49}H_{56}N_4O_3$ (%): Calculated: C, 78.58; H, 7.54; N, 7.48. Found: C, 78.62; H, 7.56; N, 7.46. HRMS (ESI) calcd. for **BOS** ($C_{49}H_{56}N_4O_3$) *m/z* = 748.4352, Found: 749.4405 $(M+H)^+$. IR (KBr) *υ*: 3444, 2962, 2071, 1702, 1616, 1514, 1356, 1223, 1117, 820, 756 cm^{-1}. ^1H NMR (400 M, $CDCl_3$) δ: 13.07 (s, 1H), 8.01 (d, *J* = 8.2Hz, 2H), 5.96–7.49 (m, 13H), 5.65 (d, *J* = 8.6 Hz, 1H), 5.21 (s, 1H), 3.29 (q, *J* = 6.8 Hz, 4H), 3.03 (d, *J* = 8.2 Hz, 4H), 1.29 (s, 9H), 1.22 (s, 9H), 1.11 (t, *J* = 8.6 Hz, 6H), 0.93 (t, *J* = 8.2 Hz, 6H). ^{13}C NMR (100 M, $CDCl_3$) δ: 166.2, 164.32, 158.3, 154.2, 153.3, 152.1, 147.7, 139.7, 136.9, 132.4, 132.4, 130.4, 130.1, 129.2, 129.0, 128.3, 127.8, 126.3, 126.3, 124.1, 123.7, 119.3, 118.4, 108.3, 67.9, 44.5, 35.0, 34.1, 31.5, 29.3, 12.5 (Figs. S3-S6).

2.3. Preparation of the test solution

The stock solution of **BOS** (100 μmol/L) was prepared in ethanol-water (1:9, v/v, Tris-HCl, pH =7.2). The solutions of various testing cation species were prepared from $Ca(NO_3)_2·4H_2O$, $AgNO_3$, $Mg(NO_3)_2·6H_2O$, $NaNO_3$, $Co(NO_3)_2·6H_2O$, $Cd(NO_3)_2·4H_2O$, $Zn(NO_3)_2·6H_2O$, $Cu(NO_3)_2·3H_2O$, $Mn(NO_3)_2·4H_2O$, $Hg(NO_3)_2·H_2O$, $Ni(NO_3)_2·6H_2O$, $Pb(NO_3)_2$, $Cr(NO_3)_3·9H_2O$, $Pd(NO_3)_2·2H_2O$, $Sn(NO_3)_2$, $Ba(NO_3)_2$, KNO_3, $LiNO_3$, $Fe(NO_3)_3·9H_2O$ and $Al(NO_3)_3·9H_2O$ using double distilled water. Before test, the cation solutions with different concentrations were obtained by diluting the thick solutions. The detailed experimental procedures are as follows: For the titration tests, 1 mL of the **BOS** stock solution and different amounts of Al^{3+} were mixed and diluted to 10 mL in volumetric flasks using ethanol-water (1:9 v/v, Tris-HCl, pH = 7.2) solution. For the selectivity tests, 1 mL of metal ion solution (100 μmol/L) and 1 mL of **BOS** solution (100 μmol/L) were added to a 10 mL volumetric flask and diluted with ethanol-water (1:9 v/v) solution. For the interference experiments, 1 mL of interference metal ion solution (1 mmol/L) were

added into the mixed solution containing 1 mL of **BOS** solution (100 μmol/L) and 1 mL of Al^{3+} solution (100 μmol/L).

2.4. Cytotoxicity assays

The toxicity of the probe and metal cation was assessed by using SGC-7901 living cells according to the conventional MTT assays. The 90% confluent cells were digested by 1 mL trypsin (0.25%) and seeded into a 96-well plate. Cells were culturing in a mixed medium of Dulbecco's modified eagle medium (DMEM) and 10% fetal bovine serum (FBS) at 37 °C under a humid environment including 5% CO_2 for 24 h. Then, the cells were treated with different concentrations of **BOS** and Al^{3+} for another 24 h, respectively. After that, the medium was removed and washed with phosphate buffered saline (PBS) for three times. Then the medium was replaced with the mixed solution of MTT (5 mg/mL) and culture medium, and incubated for an additional 4 h. Following this, the MTT was removed and washed three times with PBS. Subsequently, 150 μL DMSO was carefully added to each tube and processed by ultrasonic oscillation for 10 minutes. All the experiments were conducted in triplicate. The cell viability (%) was calculated according to the Equation: Cell viability (%) = [OD490(sample) / OD490(control)] ×100%, where OD490(sample) represents the optical density of the wells treated with various concentration of probe or metal ions and OD490(control) represents that of the wells treated with ethanol.

2.5. Cell culture and fluorescence imaging

The SGC-7901 living cells (human gastric carcinoma cells) were cultured in DMEM supplemented with 10% FBS. Before the experiments, the cells were pretreated by **BOS** (10 μmol/L) for 1 h at 37 °C in humidified air with 5% CO_2, washed three times with PBS and images were obtained. After incubation with Al^{3+} (10 μmol/L) for another 1.5 h at 37 °C, the cells were washed three times with PBS to remove remaining Al^{3+} before imaging. Confocal fluorescence imaging was carried out on Olympus FV1000 laser scanning microscope with 80× objective lens.

3. Results and discussion

3.1. Spectroscopic properties

The spectroscopic properties were explored in both fluorescence and absorption spectra thoroughly. And the results indicated that the probe showed remarkable selectivity and sensitivity for the detection of Al^{3+} in ethanol-water (v/v = 1:9). As can be seen in Fig. 1a, the reaction of **BOS** (10 μmol/L) with Al^{3+} underwent a noticeable color change from colourless to peach-red, while no change in color was found when reacting with other metal cations. Similar results also could be observed when irradiated under a fluorescent light (365 nm), the **BOS** reacting with Al^{3+} caused a dramatic color change from colourless to bright yellow (Fig. 1b). Therefore, the **BOS** owned high selectivity towards Al^{3+} and could be successfully utilized as "naked-eye" probe for Al^{3+} detection.

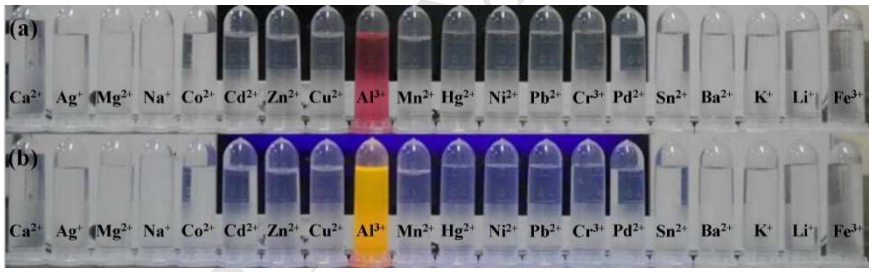

Fig. 1. Visual color (a) and fluorescence (b) change of the ethanol-water solution of **BOS** upon the addition of different metal ions.

The sensitivity of **BOS** towards Al^{3+} was checked by the fluorescence titration experiments. As depicted in Fig. 2a, because of the special spirolactam structure of the free **BOS**, no fluorescence emission was detected in the wavelength range of 570 – 700 nm. Nevertheless, when Al^{3+} was gradually added from 0 to 1.0 equiv, the emission intensity remarkably increased at 595 nm, which indicated that the xanthene moiety was interfered by the delocalization effect, and **BOS** was a ture "off-on" sensor toward Al^{3+}. No significant change in the fluorescence intensity was observed with further addition of Al^{3+} (up to 1.25 equiv), which is about 105 times than that of

the free **BOS** (Fig. 2b). The remarkable fluorescence enhancement implied that the ring-opening of spirolactam or the inhibition of the rotation of the "C=N" bond occurred with the gradual addition of Al^{3+}, and a delocalized π-conjugated moiety established eventually.

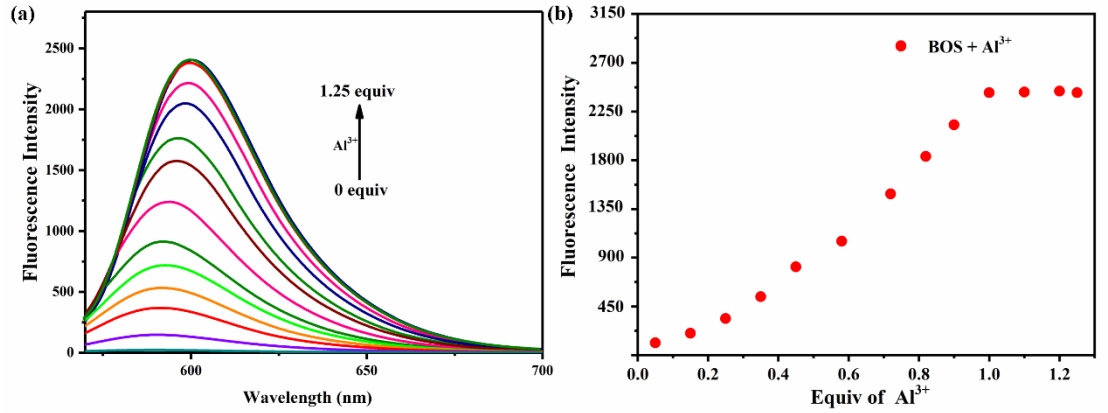

Fig. 2. (a) Fluorescence spectra of **BOS** (10 μmol/L) and (b) the changes of the fluorescence intensity at 595nm with the addition of different concentrations of Al^{3+} (0-1.25 equiv) in ethanol-water (1:9, v/v, Tris-HCl, pH =7.2) solution.

The results of the titration experiment were analyzed to figure out the quantitative relationship between the emission intensity of **BOS** and the Al^{3+} concentration. And the association constant *K* of **BOS** with Al^{3+} was determined to be $4.204*10^4$ L/mol through the Benesi-Hildebrand equation: $(F_{max}-F_0) / (F_x-F_0) = 1 + (1/K) (1/[Al^{3+}])$, where F_{max}, F_0 and F_x are the fluorescence intensities of probe in the presence of Al^{3+} at saturation, free probe, and any intermediate Al^{3+} concentration, respectively (Fig. 3a). Additionally, the detection limit of **BOS** was further determined from the above results. As shown in Fig. 3b, according to the widely used method [25,26], linear regression curve was fitted based on the plots of $(F_{min} - F_x) / (F_{min} - F_{max})$ *vs* $\log[Al^{3+}]$, in which the F_x is the emission intensity at various concentration of Al^{3+}, F_{min} and F_{max} are respectively the minimum and maximum fluorescence intensity at 595 nm. After fitting the data, the intercept of the line at x-axis was recorded as the detection limit of 1.855 μmol/L.

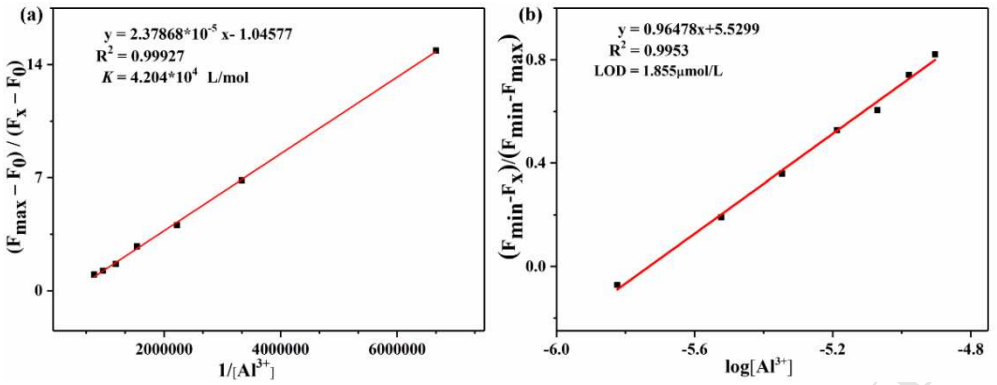

Fig. 3. (a) Benesi–Hildebrand plot of **BOS** using 1:1 stoichiometry for association. (b) The plot of $(F_{min} - F_x) / (F_{min} - F_{max})$ versus log[Al^{3+}] for the probe **BOS**.

The selectivity and anti-interference performance of probe are significant for its application. Hence, the fluorescence response of **BOS** (10 μmol/L) towards Al^{3+} ions and other various metal ions in ethanol-water (1:9 v/v, Tris-HCl, pH =7.2) was investigated. As shown in Fig. 4a, the free **BOS** exhibited negligible fluorescence emission. When different metal cations (Mn^{2+}, Pb^{2+}, Cd^{2+}, Co^{2+}, Fe^{3+}, Al^{3+}, Cu^{2+}, Ni^{2+}, Ag^{+}, Zn^{2+}, Cr^{3+}, Hg^{2+}, Pd^{2+}, Sn^{2+}, K^{+}, Li^{+}, Na^{+}, Ca^{2+}, Mg^{2+}, Ba^{2+}) were added into the **BOS** system, only Al^{3+} caused a significant fluorescence enhancement at 595nm, and no obvious fluorescence signals were detected for other ions, indicating the good selectivity of **BOS** as Al^{3+} sensor. For the interference experiment (Fig. 4b), when 10.0 equiv of competitive ions (K^{+}, Li^{+}, Na^{+}, Ca^{2+}, Mg^{2+}, Ba^{2+}, Mn^{2+}, Pb^{2+}, Cd^{2+}, Co^{2+}, Fe^{3+}, Cu^{2+}, Ni^{2+}, Ag^{+}, Zn^{2+}, Cr^{3+}, Hg^{2+}, Pd^{2+}, Sn^{2+}) were respectively added into the **BOS** test solutions, almost no change in emission intensity was found. On the contrary, upon the further addition of 1.0 equiv of Al^{3+}, a rapid fluorescence enhancement occurred, which suggested that the sensing response of **BOS** to Al^{3+} could hardly be influenced by other coexisting metal ions. The characteristics of high selectivity and sensitivity as well as the excellent anti-interference performance enabled **BOS** to be potentially used for Al^{3+} ions detection in complex systems.

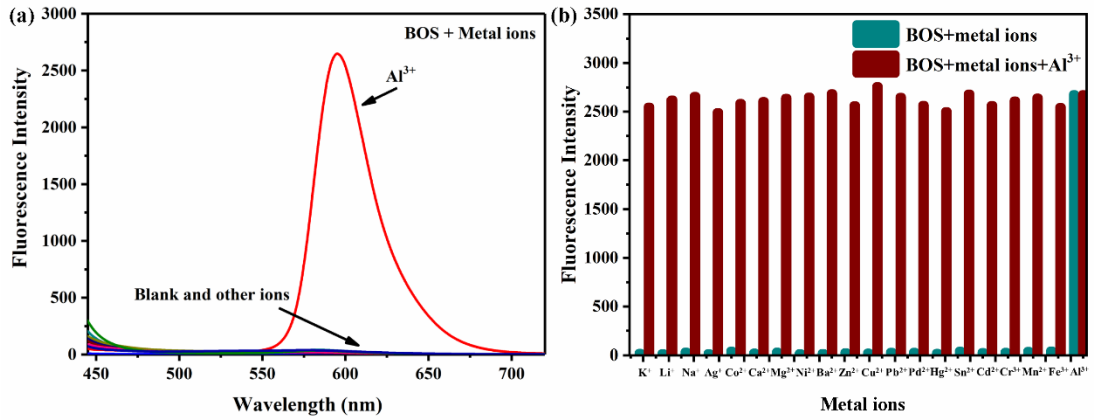

Fig. 4. (a) Fluorescence spectra of **BOS** (10 μmol/L) in ethanol-water (1:9, v/v, Tris-HCl, pH =7.2) solution upon the addition of different metal ions (10 μmol/L). (b) The emission intensities of **BOS** (10 μmol/L) at 595 nm in the presence of 10.0 equiv of different interference metal ions (dark cyan bars) or when 1.0 equiv of Al^{3+} coexiting with 10.0 equiv of competing ions added (wine bars).

The Al^{3+} sensing ability of **BOS** was also examined by UV-vis spectroscopy experiment. As depicted in Fig. S7, the titration experiments indicated that the absorption intensity markedly increased at 568 nm upon the gradual addition of Al^{3+} from 0 to 1.0 equiv. Similarly, the absorption intensity stayed still with the concentration of Al^{3+} further increasing to 1.25 equiv, suggesting a possible 1:1 binding. The different absorption intensities were detected to explore the selectivity by mixing **BOS** with the above-mentioned 20 kinds of distinct metal ions. Only the **BOS**-Al^{3+} system displayed a remarkable absorption enhancement, whereas negligible changes could be found in other test systems (Fig. S8). The results confirmed the excellent selectivity of **BOS** for Al^{3+}. For the application in complex biological environments, the probes with low background interference are preferred. Therefore, the interference experiments were illustrated by mixing **BOS** (10 μmol/L) with 10.0 equiv of interference metal ions in the presence or absence of 1.0 equiv of Al^{3+} (Fig. S9). After the introduction of Al^{3+}, the significant absorption enhancement in these competitive systems further demonstrated the good anti-interference of **BOS** for Al^{3+} recognition.

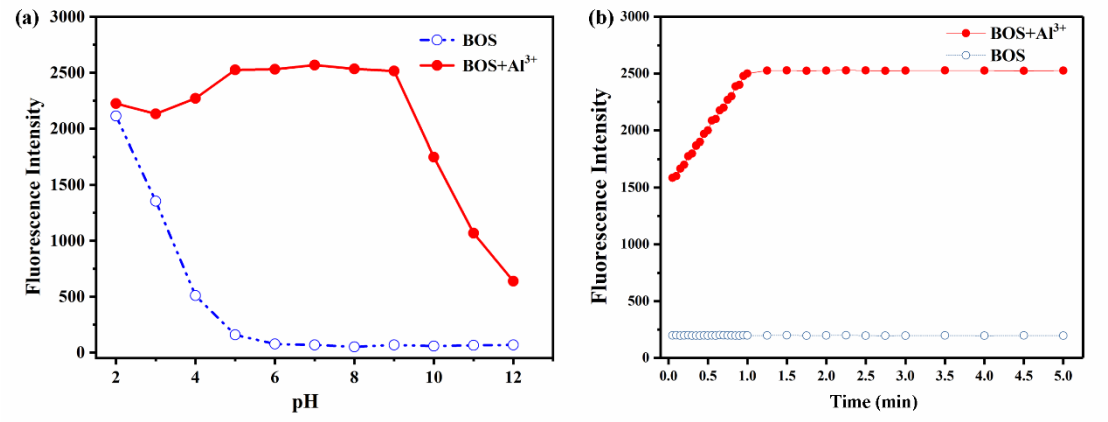

Fig. 5. Effects of pH (a) and time (b) on the Al^{3+} recognition of **BOS** (10 μmol/L) in ethanol-water (1:9, v/v, Tris-HCl, pH =7.2) solution.

Given the outstanding Al^{3+} sensing performance, **BOS** is proposed to be used in biological detection. So the effects of pH and time on the Al^{3+} response of **BOS** were further investigated through a serious of experiments. Commonly, the spirolactam ring of the rhodamine derivative opens in acidic medium and presents the fluorescence of rhodamine. As a consequence, the optimum pH conditions for **BOS** should be explored to confirm its stability in potential practical applications. In the presence or absence of Al^{3+}, the pH dependent fluorescence responses of **BOS** were recorded in the pH range of 2 – 12 (Fig. 5a). When pH < 4, both the fluorescence intensities of **BOS** and **BOS**-Al^{3+} species were strong enough because of the ring-opening of spirolactam induced by the strong protonation of the tertiary amine-N atom in acid conditions. The free **BOS** showed negligible emission when pH > 5, while strong emissions were detected after the addition of Al^{3+} within the pH value range from 5 to 9. When the pH value was greater than 9, the emissions of **BOS**-Al^{3+} were rapidly quenched due to the formation of $Al(OH)_3$ and the regeneration of spirolactam ring. The results suggested that the response of **BOS** to Al^{3+} worked well in a suitable pH region of 5 – 9 that approximated the physiological environment.

Response time is also a key index for chemosensors. The time-dependent fluorescence responses of **BOS** towards Al^{3+} were proceed in a simulated in vivo environment (ethanol-water = 1:9, v/v, Tris-HCl, pH = 7.2) at ambient temperature. With the addition of Al^{3+}, the emissions of **BOS** at 595 nm remarkably increased to

the maximum value at 57 seconds and remained unchanged in the subsequent time (Fig. 5b), revealing that **BOS** is a promising instantaneously responsive colorimetric sensor for Al^{3+}.

3.2. Cytotoxicity assays and biological imaging applications

Cytotoxicity experiments are crucial to the application of probes in biological environment [27], and MTT assays were operated on SGC-7901 living cells to investigate the biotoxicity of **BOS** and Al^{3+}. As illustrated in Fig. 6 and Table S1, the cell viability decreased slowly with the increase of the concentration of **BOS** or Al^{3+}, and the viability still stayed above 85% when 25 μmol/L **BOS** or Al^{3+} treated, which showed that **BOS** was low cytotoxic to living cells and suitable for bioimaging.

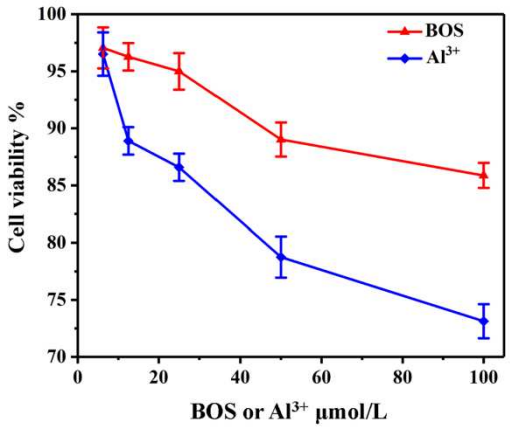

Fig. 6. SGC-7901 living cells viability of **BOS** and Al^{3+} quantified by the MTT assay.

So the fluorescence imaging experiments were carried out in SGC-7901 cells. As expected, free **BOS** presented no detectable fluorescence signals in cells without Al^{3+} (Fig. 7a), and bright fluorescence signals were observed after the incubation **BOS** with Al^{3+} (Fig. 7c). Bright-field transmission images of cells treated with **BOS**-Al^{3+} indicated that the cells were viable during the imaging experiments (Fig. 7b). These results revealed that **BOS** could readily penetrate the cell membrane and be used for in vitro imaging of Al^{3+} in living cells.

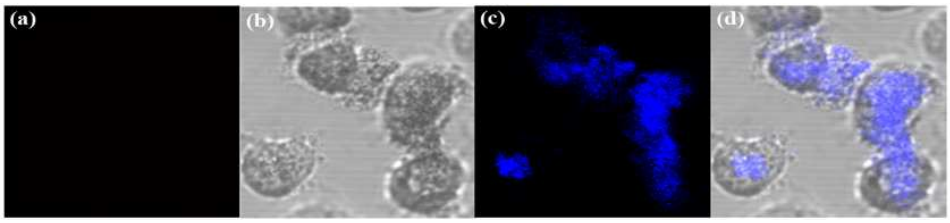

Fig. 7. The fluorescence images and of SGC-7901 cells treated with **BOS** (20 μmol/L) either in absence (**a**) or presence (**c**) of 20 μmol/L Al^{3+} for 1h at 37 °C, and the bright-field image of cells shown in panel (**b**) as well as the overlay image (**d**) of (**b**) and (**c**).

*3.5. Probable mechanism for the interactions of **BOS** with Al^{3+}*

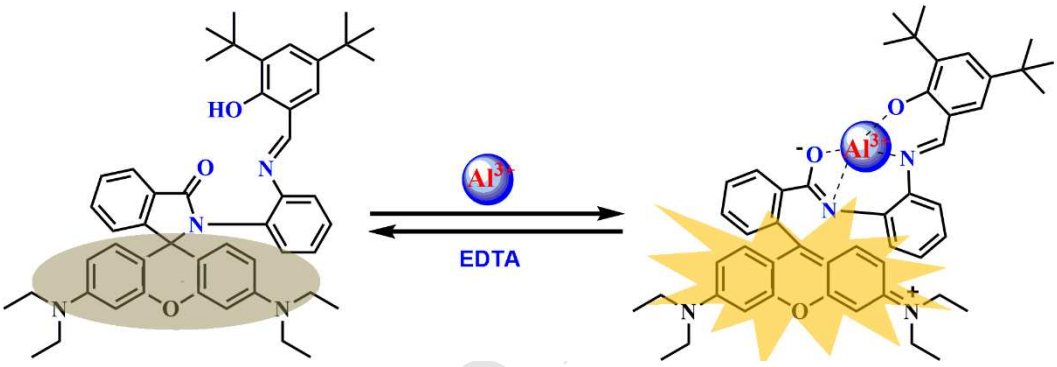

Fig. 8. The Al^{3+}-sensing mechanism of **BOS**.

Based on the spectral response of **BOS** to Al^{3+}, the possible sensing mechanism should be due to the chelation-induced ring opening of rhodamine spirolactam (Fig. 8). To be more specific, a conjugated moiety was generated when the multidentate coordination sites (carbonyl and hydroxy oxygen atoms as well as imino nitrogen atoms) chelated Al^{3+}, and at the same time the spirolactam ring was induced to be opened, exhibiting remarkable fluorescence enhancements [28,29].

As displayed in Fig. S10, binding analysis was carried out by using the continuous variations with a total concentration of [**BOS**] + [Al^{3+}] as 10 μmol/L to determine the binding stoichiometry between them (Job's plot) [30,31]. The fluorescence emission intensity showed a maximum at 595 nm when the mole fraction of Al^{3+} approached 0.5, which demonstrated the 1:1 binding stoichiometry of

Al^{3+}–**BOS**.

EDTA was added into the **BOS**-Al^{3+} system to test the binding reversibility of **BOS**. As shown in Figs. S11 and S12, after the introduction of EDTA, the intensities of fluorescence and absorbance rapidly decreased with the fluorescent color changing from bright yellow to colorless, while the spectral signals recovered with the addition of Al^{3+} again (Fig. S12). The decreasing-reproducing processes of fluorescence intensity can be repeated several cycles without obvious changes, suggesting that **BOS** is a true reversible probe for Al^{3+}.

4. Conclusion

A novel chromo-fluorogenic probe **BOS** displaying specific color change and fluorescence response towards Al^{3+} was designed, synthesized and characterized. The probe shows good selectivity and high sensitivity towards Al^{3+} *via* a 1:1 binding mode in ethanol-water solution over a wide range of tested metal ions. The "turn on" fluorescence response produced by the chelation-induced ring opening of spirolactam indicates that **BOS** can be applied to rapid "naked-eyes" Al^{3+} detection in the pH range of 5 – 9. Fluorescence imaging of Al^{3+} in SGC-7901 living cell suggests that this probe is promising for the practical applications to Al^{3+} ion assays in environmental and biological samples.

Acknowledgements

This work was supported by the National Natural Science Foundation of China (Grant Nos. 21703135 and 21803042), the Natural Science Foundation of Shaanxi Province (No. 2019JQ-249), the Natural Science Foundation of the Department of Education of Shaanxi Province (No. 17JS034), the Outstanding Young Talents Fund of University in Shaanxi Province (No. 18SKY001) and the Doctoral Scientific Research Starting Foundation of Shangluo University (No. 17SKY028).

References

[1] F. Carson, S. Agrawal, M. Gustafsson, A. Bartoszewicz, F. Moraga, X. Zou, B. Martín-Matute, Ruthenium complexation in an aluminium metal–organic framework and its application in alcohol oxidation catalysis, Chem. Eur. J. 18 (2012) 15337-15344.

[2] J. Hirsch, Aluminium in innovative light-weight car design, Mater. Trans. 52 (2011) 818-824.

[3] Y.K. Jang, U.C. Nam, H.L. Kwon, I.H. Hwang, C. Kim, A selective colorimetric and fluorescent chemosensor based-on naphthol for detection of Al^{3+} and Cu^{2+}, Dyes Pigm. 99 (2013) 6-13.

[4] N. Murer, R. Oltra, B. Vuillemin, O. Néel, Numerical modelling of the galvanic coupling in aluminium alloys: a discussion on the application of local probe techniques, Corros. Sci. 52 (2010) 130-139.

[5] Rodiansono, T. Hara, N. Ichikuni, S. Shimazu, A novel preparation method of Ni–Sn alloy catalysts supported on aluminium hydroxide: application to chemoselective hydrogenation of unsaturated carbonyl compounds, Chem. Lett. 41 (2012) 769-771.

[6] R. Zhang, Y. Liu, M. He, Y. Su, X. Zhao, M. Elimelech, Z. Jiang, Antifouling membranes for sustainable water purification: strategies and mechanisms, Chem. Soc. Rev. 45 (2016) 5888-5924.

[7] M.C. Lin, M. Gong, B. Lu, Y. Wu, D.Y. Wang, M. Guan, M. Angell, C. Chen, J. Yang, B.J. Hwang, H. Dai, An ultrafast rechargeable aluminium-ion battery, Nature 520 (2015) 324-328.

[8] C. Samorì, D. Cespi, P. Blair, P. Galletti, D. Malferrari, F. Passarini, I. Vassura, E. Tagliavini, Application of switchable hydrophilicity solvents for recycling multilayer packaging materials, Green Chem. 19 (2017) 1714-1720.

[9] M. Ogimoto, K. Suzuki, N. Haneishi, Y. Kikuchi, M. Takanashi, N. Tomioka, Y. Uematsu, K. Monma, Aluminium content of foods originating from aluminium-containing food additives, Food Addit. Contam., Part B 9 (2016) 185-190.

[10] A. Mirza, A. King, C. Troakes, C. Exley, Aluminium in brain tissue in familial alzheimer's disease, J. Trace Elem. Med Biol. 40 (2017) 30-36.

[11] A.J. Thenmozhi, T.R.W. Raja, U. Janakiraman, T.J.N.R. Manivasagam, Neuroprotective effect of hesperidin on aluminium chloride induced alzheimer's disease in wistar rats, Neurochem. Res. 40 (2015) 767-776.

[12] M. Haouas, F. Taulelle, C. Martineau, Recent advances in application of ^{27}Al NMR spectroscopy to materials science, Prog. Nucl. Magn. Reson. Spectrosc. 94-95 (2016) 11-36.

[13] S. Zeng, S.J. Li, X.J. Sun, M.Q. Li, Y.Q. Ma, Z.Y. Xing, J.L. Li, A naphthalene-quinoline based chemosensor for fluorescent "turn-on" and absorbance-ratiometric detection of Al^{3+} and its application in cells imaging, spectrochim. Acta, Part A 205 (2018) 276-286.

[14] X. Hu, X. Mao, X. Zhang, Y. Huang, One-step synthesis of orange fluorescent copper nanoclusters for sensitive and selective sensing of Al^{3+} ions in food samples, Sens. Actuators, B 247 (2017) 312-318.

[15] S. Gui, Y. Huang, F. Hu, Y. Jin, G. Zhang, L. Yan, D. Zhang, R. Zhao, Fluorescence turn-on chemosensor for highly selective and sensitive detection and bioimaging of Al^{3+} in living cells based on ion-induced aggregation, Anal. Chem. 87 (2015) 1470-1474.

[16] Z. Zhang, Y. Miao, L. Lian, G. Yan, Detection of quercetin based on Al^{3+}-amplified phosphorescence signals of manganese-doped ZnS quantum dots, Anal. Biochem. 489 (2015) 17-24.

[17] S. Sinha, B. Chowdhury, P. Ghosh, A highly sensitive esipt-based ratiometric fluorescence sensor for selective detection of Al^{3+}, Inorg. Chem. 55 (2016) 9212-9220.

[18] V.K. Gupta, N. Mergu, L.K. Kumawat, A.K. Singh, A reversible fluorescence "Off–On–Off" sensor for sequential detection of aluminum and acetate/fluoride ions, Talanta 144 (2015) 80-89.

[19] M.H. Lee, J.S. Kim, J.L. Sessler, Small molecule-based ratiometric fluorescence probes for cations, anions, and biomolecules, Chem. Soc. Rev. 44 (2015) 4185-4191.

[20] X.L. Shi, G.J. Mao, X.B. Zhang, H.W. Liu, Y.J. Gong, Y.X. Wu, L.Y. Zhou, J. Zhang, W. Tan, Rhodamine-based fluorescent probe for direct bio-imaging of lysosomal pH changes, Talanta 130 (2014) 356-362.

[21] O. Sunnapu, N.G. Kotla, B. Maddiboyina, G.S. Asthana, J. Shanmugapriya, K. Sekar, S. Singaravadivel, G. Sivaraman, Rhodamine based effective chemosensor for chromium(III) and their application in live cell imaging, Sens. Actuators, B 246 (2017) 761-768.

[22] C. Chang, F. Wang, J. Qiang, Z. Zhang, Y. Chen, W. Zhang, Y. Wang, X. Chen, Benzothiazole-based fluorescent sensor for hypochlorite detection and its application for biological imaging, Sens. Actuators, B 243 (2017) 22-28.

[23] V.S. Lin, W. Chen, M. Xian, C.J. Chang, Chemical probes for molecular imaging and detection of hydrogen sulfide and reactive sulfur species in biological systems, Chem. Soc. Rev. 44 (2015) 4596-4618.

[24] S.L. Shen, X.P. Chen, X.F. Zhang, J.Y. Miao, B.X. Zhao, A rhodamine B-based lysosomal pH probe, J. Mater. Chem. B 3 (2015) 919-925.

[25] A. Caballero, R. Martínez, V. Lloveras, I. Ratera, J. Vidal-Gancedo, K. Wurst, A. Tárraga, P. Molina and J. Veciana, Highly selective chromogenic and redox or fluorescent sensors of Hg^{2+} in aqueous environment based on 1,4-disubstituted azines, J.Am. Chem. Soc. 127 (2005) 15666-15667.

[26] J. Wang, L. Long, D. Xie, X. Song, Cu^{2+}-selective "off–on" chemsensor based on the rhodamine derivative bearing 8-hydroxyquinoline moiety and its application in live cell imaging, Sensors Actuators B:Chem. 177 (2013) 27-33.

[27] M. Maszewska, J. Leclaire, M. Cieslak, B. Nawrot, A. Okruszek, A.M. Caminade, J.P. Majoral, Water-soluble polycationic dendrimers with a phosphoramidothioate backbone: preliminary studies of cytotoxicity and oligonucleotide/plasmid delivery in human cell culture, Oligonucleotides 13 (2003) 193-205.

[28] H.S. Kim, S. Angupillai, Y.A. Son, A dual chemosensor for both Cu^{2+} and Al^{3+}: a potential Cu^{2+} and Al^{3+} switched YES logic function with an INHIBIT logic gate

and a novel solid sensor for detection and extraction of Al^{3+} ions from aqueous solution, Sens. Actuators, B 222 (2016) 447-458.

[29] M. Beija, C.A.M. Afonso, J.M.G. Martinho, Synthesis and applications of rhodamine derivatives as fluorescent probes, Chem. Soc. Rev. 38 (2009) 2410-2433.

[30] V. Luxami, Renukamal, K. Paul, S. Kumar, A dual-responsive chromo-fluorescent probe for detection of Zn^{2+} and Fe^{3+} via two different approaches, RSC Adv. 3 (2013) 9189-9192.

[31] K. Boonkitpatarakul, J. Wang, N. Niamnont, B. Liu, L. McDonald, Y. Pang, M. Sukwattanasinitt, Novel turn-on fluorescent sensors with mega stokes shifts for dual detection of Al^{3+} and Zn^{2+}, ACS Sens. 1 (2016) 144-150.

1. A novel rhodamine-based probe **BOS** is designed and synthesized.
2. **BOS** is able to high selectively and sensitively detect Al^{3+}.
3. The detection process can be identified through naked eye.
4. **BOS** is capable of detecting Al^{3+} in complex biological environment.